Table VIII. Effective Magnetic Moments of Selected Vanadium Oxygen Clusters with Varying Numbers of V(IV) d^1 Sites

anion	no. of V(IV) centers	μ_{eff}/μ_B per V(IV)[a]	V(IV)···V(IV)[b]	ref
$[V_{14}AsO_{40}]^{7-}$	2	1.77	8.72	57
$[V_{12}As_8O_{40}(HCO)_2]^{3-}$	6	1.75	5.25	12g
$[V_{12}As_8O_{40}(HCO)_2]^{5-}$	8	1.39	c	12g
$[V_{14}As_8O_{42}(SO_3)]^{6-}$	14	1.20	2.81-3.06	58
$[V_6O_{11}(OH)_2\{(OCH_2)_3CCH_3\}_2]^{2-}$	2	1.84	-	this work
$[V_6O_9(OH)_4\{(OCH_2)_3CCH_3\}_2]^{2-}$	4	1.74	3.20-4.60	this work
$[V_6O_7(OH)_6\{(OCH_2)_3CCH_3\}_2]^{2-}$	6	1.25	3.25-4.60	this work

[a] Room temperature. [b] Distances in Å. [c] Complicated intermediate region where the number of formal V(IV) sites is greater than half the total number of V centers.

The magnetic behavior of **5c**, **6**, and **7** is qualitatively similar to that reported for other vanadium-oxygen clusters with varying numbers of V(IV) d^1 centers (Table VIII). In species with a small number of spins, V(IV) d^1 sites, the spins may be trapped and remain as far apart as possible, resulting in nearly spin-only values for μ_{eff} per V(IV). Spin-spin coupling increases with an increasing number of V(IV) centers, which necessarily results in close contacts. A more detailed analysis of the magnetic properties of these and related hexavanadium and decavanadium clusters is being developed.[56]

Conclusions

1. The hexavanadate core $\{V_6O_{19}\}$ is stabilized in the presence of alkoxy ligands. The replacement of bridging oxo groups by bridging alkoxy groups serves to reduce the cluster charge and to stabilize the hexametalate core for vanadium.

2. In the solid state and in solution, the protonation sites of both oxidized and reduced hexavanadate cores have been identified as the doubly bridging oxo groups, establishing these as more nucleophilic/basic than the terminal oxo groups.

3. The hexavanadate cluster readily undergoes coupled reduction/protonation to give the mixed-valence species $[V_6O_9(OH)_4\{(OCH_2)_3CCH_3\}_2]^{2-}$ and the V(IV) cluster $[V_6O_7(OH)_6\{(OCH_2)_3CCH_3\}_2]^{2-}$.

4. Reduction and protonation can be decoupled. Thus, electrochemical reduction of $[V_6O_{13}\{(OCH_2)_3CCH_3\}_2]^{2-}$ (**3**) gives the mixed-valence species $[V^V_5V^{IV}O_{13}\{(OCH_2)_3CCH_3\}_2]^{3-}$, while protonation of **3** yields the neutral polymetalate $[V_6O_{11}(OH)_2\{(OCH_2)_3CCH_3\}_2]$.

Acknowledgment. J.Z. thanks the National Science Foundation for support of this work (CHE8815299 and CHE9119910). Acknowledgment is also made to the donors of the Petroleum Research Fund, administered by the American Chemical Society, for partial support of this research. This work was also supported by NSF Grant BBS 8711617 (C.P.S.) and NIH Grant GM-35103 (C.P.S.). EPR analysis software was furnished by the Illinois ESR Research Center, NIH Division of Research Resources Grant No. RR01811.

Supplementary Material Available: Tables of experimental details and crystal parameters for the structures of **1-3** and **5-7** and tables of atomic positional parameters, bond lengths and angles, anisotropic temperature factors, and calculated hydrogen atom positions for the structures (60 pages); observed and calculated structure factors (135 pages). Ordering information is given on any current masthead page.

Organic Template-Directed Inorganic Crystallization: Oriented Nucleation of $BaSO_4$ under Compressed Langmuir Monolayers

Brigid R. Heywood* and Stephen Mann

Contribution from the School of Chemistry, University of Bath Claverton Down, Bath BA2 7AY, United Kingdom. *Received October 21, 1991. Revised Manuscript Received February 3, 1992*

Abstract: Langmuir monolayers of *n*-eicosyl sulfate were shown to influence the nucleation of $BaSO_4$ grown from supersaturated solutions ($S = 30$) at room temperature (293 K). Thin, elongated single crystalline plates were nucleated with the (100) face parallel to the plane of the monolayer. Partial matching of cation-cation distances with the interheadgroup spacings and stereochemical complementarity between the anionic motif and sulfate headgroups are potential factors responsible for oriented nucleation. The oriented crystals exhibited an unusual texture of coherently intergrown rhombic subunits which was attributable to monolayer-induced growth along specific lattice directions parallel to the monolayer/solution interface. By contrast, barium sulfate crystals nucleated under compressed eicosanoic acid monolayers were oriented along the [010] direction. These crystals were irregular in morphology, suggesting a kinetic rather than a structural influence of the organic template on nucleation at the monolayer/solution interface.

Introduction

Crystal formation involves two major steps: nucleation and growth. Nucleation is favored when relatively long-lived clusters are formed through the aggregation of ions and/or molecular species into stable structural configurations. Growth then proceeds through the addition of further species to nascent crystal faces of variable surface energy. In bulk solution the structure, size, and habit of the growing crystals is regulated by a multiplicity of interrelated factors, including supersaturation, pH, temperature, and the level of additives. However, despite an extensive knowledge of these factors, the development of reliable protocols for controlling crystallization remains a challenge in solid-state chemistry.

A recent development in this area involved the use of Langmuir monolayers of surfactant molecules as molecular templates for the oriented nucleation of organic and inorganic crystals.[1-11] This

* Address correspondence to this author at the Department of Chemistry and Applied Chemistry, University of Salford, Salford M5 rWT, UK.

(1) Landau, E. M.; Grayer-Wolf, S.; Levanon, M.; Leiserowitz, L.; Lahav, M.; Sagiv, J. *Mol. Cryst. Liq. Cryst.* **1986**, *134*, 323-325.
(2) Landau, E. M.; Popovitz-Bior, R.; Levanon, M.; Leiserowitz, L.; Lahav, M.; Sagiv, J. *J. Am. Chem. Soc.* **1989**, *111*, 1436-1439.

0002-7863/92/1514-4681$03.00/0

approach utilizes the potential of controlling the molecular recognition events which may exist between the incipient nuclei and organized organic assemblies. Much of the inspiration for this approach has arisen from research into the processes regulating mineral deposition in biological systems.[12,13] In many instances, biomineralization is achieved through the controlled nucleation of the inorganic crystals on a highly ordered organic substrate. The resulting biominerals exhibit species-specific structures, morphologies, and spatial organization.

Landau et al.[1,2] have shown that monomolecular films formed from resolved amino acids initiate the rapid nucleation of oriented glycine crystals at the air/water interface. The preferential alignment of the glycine crystals was only observed when structural information in the monolayer was correlated with specific lattice parameters in the nascent crystal. Similar studies have shown that compressed surfactant films of precise molecular design can induce the oriented nucleation of inorganic crystals.[1-11] For example, crystallization of calcium carbonate under stearic acid monolayers resulted in oriented calcite and vaterite crystals.[3-9] In this instance, both lattice matching and stereochemical factors were implicated in the preferential nucleation of crystal faces, while electrostatic interactions were responsible for polymorph selectivity. The complementarity between the stereochemical disposition of the headgroup carboxylates and the carbonate motif of the $\{1\bar{1}.0\}$ face was postulated as the crucial recognition process in these experiments.[7,9] In the present study, the planar carbonate motif has been exchanged for a tetrahedral anion (sulfate), in order to assess whether stereochemical factors have generic importance in monolayer-induced inorganic crystallization processes. Indeed, we find that the nucleation of $BaSO_4$ under *n*-eicosyl sulfate monolayers results in oriented crystals and can be rationalized in terms of a mechanism that depends primarily on stereochemical recognition at the organic–inorganic interface. Moreover, we show for the first time that the nanoscale architecture of the oriented crystals can be influenced by subsequent growth processes under the sulfate monolayers. An unusual and complex morphology is established through the selective interaction of developing crystal faces with the monolayer headgroups. Compressed carboxylate monolayers induced the nucleation of $BaSO_4$ on the (010) face. In this system, however, the irregular morphology of the crystals suggests that kinetic rather than structural factors are implicated in nucleation. The ability to engineer both the size, morphology, and crystallographic orientation of inorganic solids in this way has important implications for our understanding of biomineralization, and in the design of novel synthetic strategies for the tailored formation of advanced materials.

Materials and Methods

Barium sulfate was crystallized from a supersaturated solution in either the presence or absence of compressed monolayers. The supersaturated solution (degree of supersaturation (S) = 30, defined as the ratio of ion activity products (IAP) to the solubility product (K_{sp}) all to the power of one-half ($S = (IAP)/K_{sp})^{1/2}$; K_{sp} (25 °C) barium sulfate = 1.0×10^{10} mol^2 dm^6) was prepared by mixing equimolar solutions of barium chloride and sodium sulfate (3.125×10^{-4} M, pH 7.0, temp 293 K). Under these conditions the induction time (determined by light scattering techniques) exceeds 2 h at room temperature which allows for sufficient time for the application and compression of a monolayer before crystallization in bulk solution is initiated.

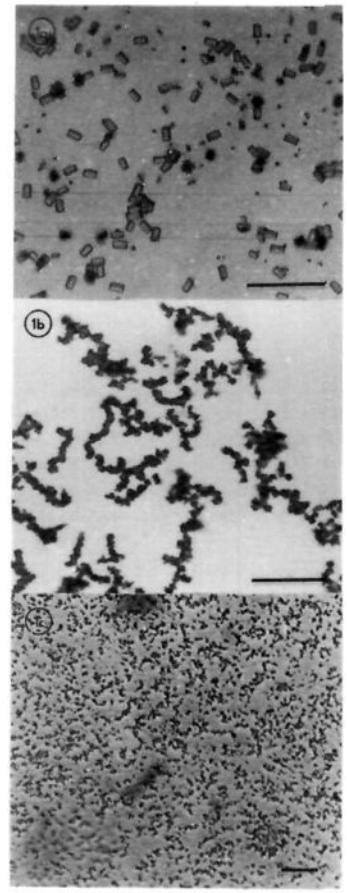

Figure 1. Optical micrographs of synthetic barium sulfate crystals collected from (a) the bottom of the reaction vessel, (b) the air/solution interface in the absence of a monolayer. (c) Optical micrograph of $BaSO_4$ crystals formed under compressed Langmuir monolayers of *n*-eicosyl sulfate. Bars = (a) 10 μm, (b) 10 μm, (c) 10 μm.

Langmuir monolayers of *n*-eicosyl sulfate ($CH_3(CH_2)_{19}OSO_3Na$) (pK_a = 1.92 (298 K)) or eicosanoic acid ($CH_3(CH_2)_{18}CO_2H$) (pK_a = 6.0) were formed at the air/solution interface of freshly prepared supersaturated barium sulfate solutions. Monomolecular films were prepared in either a Meyer Feintechnik or Nima Technology circular trough by spreading the surfactant/solvent (1 mg mL^{-1} of surfactant dissolved in hexane, chloroform, and methanol mixture (3:1:1)) over the solution surface, and then reducing the surface area to the required limit by slow compression. The monolayer phase, surface pressure, and limiting area per molecule were determined from π–A isotherms recorded during compression.

The crystals were examined in situ using a stereomicroscope (Meiji) for determinations of particle distribution and nucleation density. Samples were also removed by collection on glass coverslips for further examination by optical microscopy (Zeiss Axiophot) and for X-ray diffraction (XRD). The structure and crystallographic orientation of the crystals were analyzed by high resolution transmission electron microscopy using established procedures.[9] Crystals grown on the monolayer were collected by slowly dipping formvar-coated, carbon reinforced copper electron microscope grids (3 mm) through the monolayer. Excess fluid collected during the dipping procedure was removed immediately with absorbent paper. The grids were then allowed to dry in air. Crystals grown in the absence of a monolayer were collected on glass coverslips placed at the bottom of the reaction vessel. The crystals were generally collected after t = 8 h. In some experiments, however, the crystals were harvested at earlier times (t = 0.5 – 4 h).

All samples were examined using a JEOL 2000FX high resolution analytical transmission electron microscope (HRTEM) operating at 200

(3) Mann, S.; Heywood, B. R.; Rajam, S.; Birchall, J. D. *Nature (London)* **1988**, *334*, 692–695.
(4) Mann, S.; Heywood, B. R.; Rajam, S.; Birchall, J. D. *Proc. R. Soc. London, Ser. A* **1989**, *423*, 457–471.
(5) Mann, S.; Heywood, B. R.; Rajam, S.; Walker, J. B. W. *Surface Reactive Peptides and Polymers*; American Chemical Society: Washington, DC, 1989.
(6) Mann, S.; Heywood, B. R.; Rajam, S.; Walker, J. B. W.; Davey, R. J.; Birchall, J. D. *Adv. Mater.* **1990**, *2*(05), 257–261.
(7) Mann, S.; Heywood, B. R.; Rajam, S.; Walker, J. B. W. *J. Phys. D: Appl. Phys.* **1991**, *3*, 154–164.
(8) Rajam, S.; Heywood, B. R.; Walker, J. B. A.; Mann, S.; Davey, R. J.; Birchall, J. D. *J. Chem. Soc., Faraday Trans.* **1991**, *87*(5), 727–734.
(9) Heywood, B. R.; Rajam, S.; Mann, S. Oriented Crystallization of $CaCO_3$ under Compressed Monolayers. Part 2. *J. Chem. Soc., Faraday Trans.* **1991**, *87*(5), 735–743.
(10) Zhao, X. K.; Xu, S.; Fendler, J. H. *Langmuir* **1991**, *7*, 520–523.
(11) Gavish, M.; Popovitz-Bior, R.; Lahav, M.; Leiserowitz, L. *Science* **1990**, *250*, 973–974.
(12) Addadi, L.; Weiner, S. *Proc. Natl. Acad. Sci. U.S.A.* **1985**, *82*, 4110–4113.
(13) Mann, S., Webb, J., Williams, R. J. P., Eds.; *Biomineralization: Chemical and Biochemical Perspectives*; VCH Publishers: Weinheim, 1989.

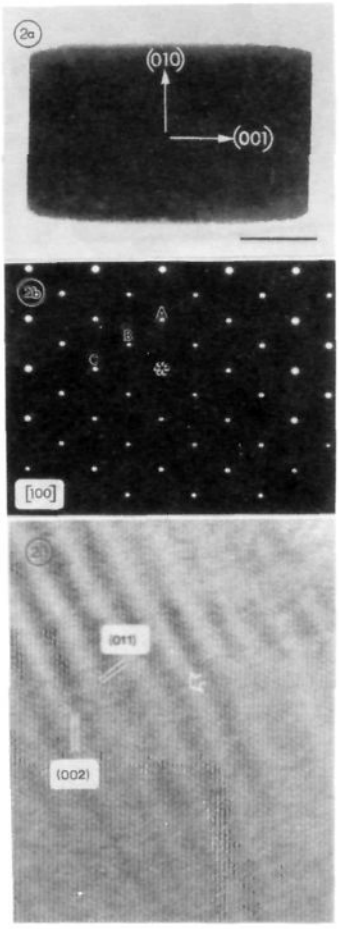

Figure 2. (a) Transmission electron micrograph of synthetic barium sulfate crystals collected from the bottom of the crystallization vessel in the absence of a monolayer. Bar = 500 nm. (b) Single-crystal electron diffraction pattern from the particle imaged in (a). The pattern corresponds to the [100] zone of baryte: reflection A = (020) = 0.273 nm, B = (011) = 0.434 nm, C = (002) = 0.358 nm; angles (020) ∧ (002) = 90°, (020) ∧ (011) = 37°. (c) HRTEM image of a synthetic baryte crystal lying perpendicular to the [100] zone axis showing (002) (0.358 nm) and (011) (0.434 nm) lattice fringes. A number of larger periodic bands (→) are also evident.

kV. Selected area electron diffraction data were recorded from individual crystals. The electron diffraction patterns and lattice images were indexed by comparing their *d*-spacings and interplanar angles with calculated values assuming, for barium sulfate ($BaSO_4$), an orthorhombic unit cell (space group *Pnma*) with unit cell dimensions a_o = 0.8878 nm, b_o = 0.5450 nm, c_o = 0.7152 nm.[14]

Results

Control Crystals. In the absence of a monolayer, the majority of crystals were located at the bottom of the crystallization vessel as a result of sedimentation (Figure 1a). Precipitation at the air/solution interface was negligible although small aggregates of crystals were collected occasionally from the surface (Figure 1b). These crystal were extensively intergrown and consistently smaller than particles collected from the bottom of the reaction vessel.

TEM examination showed the control crystals to be rectangular tablets of homogeneous size distribution (mean length = 3.7 mm, s = 670 nm) (Figure 2a). The mean aspect ratio was 1.5 (s = 0.13). Single-crystal electron diffraction patterns obtained from individual crystals indicated that they were elongated along the [001] crystallographic axis and terminated by well-defined (001) faces (Figure 2b). The large top and bottom faces were noticeably

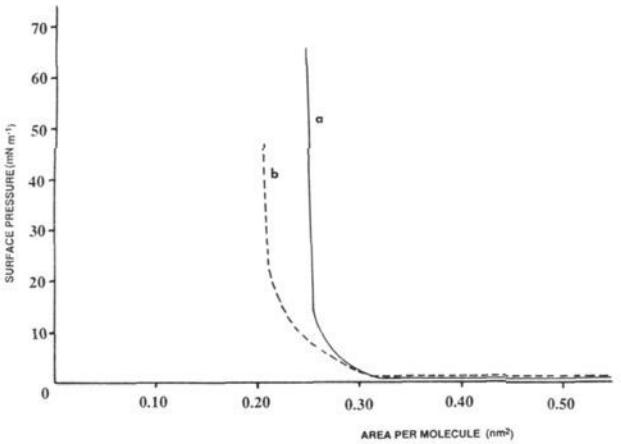

Figure 3. π–A isotherms for monolayers on 0.01 M NaCl subphase pH 7.0 containing Ba^{2+} (1.5×10^{-4} M) (a) *n*-eicosyl sulfate, (b) eicosanoic acid.

rounded rather than smooth, suggesting that these surfaces were of composite form of general index {*hk*0}.

Analyses of the electron diffraction patterns indicated that the control crystals were highly ordered (Figure 2b). The reflections were well defined with no evidence of texture patterns, streaking, or additional reflections. HRTEM studies of the control crystals confirmed these observations (Figure 2c). Coherent well-defined lattice fringes were readily imaged. The thinness of the crystals resulted in dense periodic bands (24–28 Å) along the edges of some particles as a result of the bending distortions under the electron beam.

Monolayer-Grown Crystals. Figure 3 shows surface-pressure isotherms recorded for *n*-eicosyl sulfate and eicosanoic acid spread on subphases supersaturated in $BaSO_4$ at 293 K. Under these conditions, the sulfate monolayer was stable in the solid phase even at low surface pressures (10 mN m^{-1}). Once formed, the monolayers were shown to be stable for long periods (>8 h). Collapse of the alkyl sulfate monolayers occurred in the range of 55–57 mN m^{-1}, and the limiting area per molecule was 26 Å^2. Compressed eicosanoic acid monolayers collapsed at 43 – 47 mN m^{-1}, and their limiting area per molecule was 22 – 24 Å^2. The presence of Ba^{2+} in the solution subphase caused only a minimal expansion of the sulfate monolayer (Figure 3). This observation was in agreement with earlier work[16–19] and indicated that the condensing effect of barium ions, noted for carboxylate monolayers,[20] was absent.

In the presence of a sulfate monolayer, the crystallization induction time (determined by light scattering techniques) was reduced from 2.5 h to <1 h, and the pattern of precipitation changed dramatically. Crystallization was confined almost exclusively to the monolayer/solution interface where a dense sheet of $BaSO_4$ crystals was formed (Figure 1c). A typical nucleation density was 2.1×10^6 crystals/mm^2. The crystals were smaller than those formed in the control experiments (mean length = 670 nm, s = 70 nm). Viewed in TEM, individual crystals were thin anisotropic plates with an increased aspect ratio (1.7) compared with the control sample (Figures 4a and 5a). Each monolayer-nucleated crystal showed nanoscale texture consisting of an interconnecting mosaic of diamond-shaped (angles 74° and 106°) and rectangular subunits. The rhombic domains were located in the central region of the crystals and were smaller (20–40 nm) than the rectangular units sited at the periphery of the plates. Some crystals appeared perforated due to incomplete intergrowth of these two domain types (Figures 4a and 5a). Despite this

(14) Hill, R. J. *Can. J. Mineral.* **1977**, *15*, 525–529.
(15) Stenhagen, E. *Trans. Faraday Soc.* **1950**, *36*, 496–499.
(16) Betts, J. J.; Pethica, B. A. *Trans. Faraday Soc.* **1956**, *52*, 1581–1589.
(17) Phillips, J. N.; Rideal, E. *Discuss. Faraday Soc.* **1955**, *232*, 159–172.
(18) Goddard, E. D. *Adv. Colloid Interface Sci.* **1974**, *4*, 45–79.
(19) Goddard, E. D.; Kao, O.; Kung, H. C. *J. Colloid Interface Sci.* **1968**, *27*(4), 616–624.
(20) Bloch, J. M.; Yun, W. *Phys. Rev. A* **1990**, *41*(2), 844–849.

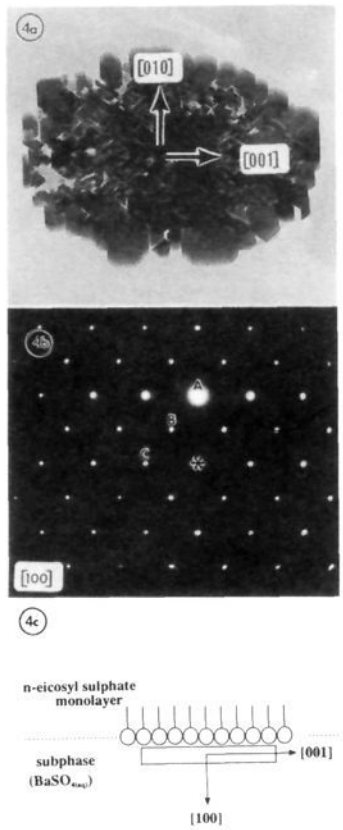

Figure 4. (a) TEM image of barium sulfate crystal nucleated under an *n*-eicosyl sulfate monolayer. Bar = 10 nm. (b) Single-crystal electron diffraction pattern from crystal imaged in (a). The diffraction pattern corresponds to the [100] zone of barium sulfate: reflection A = 0.273 nm (020), B = 0.434 nm (011), C = 0.358 nm (002). Angles (020) ∧ (002) = 90°, (020) ∧ (011) = 37°. (c) Schematic showing the relationship between the morphology of the crystal and its crystallographic orientation relative to the monolayer.

complex architecture, electron diffraction patterns obtained from individual particles showed them to be single crystals of barium sulfate (Figure 4b). This was confirmed by lattice images of the monolayer-grown crystals which showed coherent fringes across the domain boundaries in individual crystals (Figure 5b).

The electron diffraction patterns recorded from *n*-eicosyl sulfate monolayer-nucleated crystals invariably corresponded to the [100] crystallographic zone indicating that the (100) face of $BaSO_4$ was aligned parallel to the monolayer surface (Figure 4, a and c). As for the control crystals, the axis of elongation was [001] with the [010] direction parallel to the crystal width. The edges of the diamond-shaped subunits were indexed as {011} side faces while the rectangular domains were bounded by (001), {011}, and (010) edges.

It is noteworthy that in a number of cases the electron diffraction patterns were distinguished by the occurrence of discrete satellite spots (triplets and doublets). Furthermore, additional reflections (e.g., (001), (003), (005)), which were inconsistent with the conditions defined by the relevant structure factors, appeared in some patterns (Figure 6). At the present time it is unclear whether these additional reflections can be attributed solely to double diffraction,[21] since the excitation of non-allowed diffraction spots may be indicative of (1) the mosaic texture of the crystals or (2) a lowering of the crystal symmetry.[22]

Monolayers of eicosanoic acid in the solid phase also induced barium sulfate crystallization at the interface (Figure 7a). In this case, however, the induction time was increased (1.5 – 2 h)

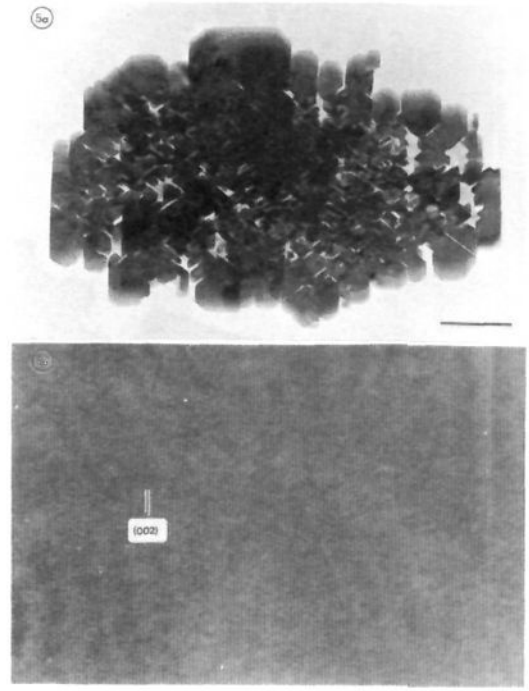

Figure 5. (a) TEM micrograph of barium sulfate crystal grown under a compressed monolayer of *n*-eicosyl sulfate showing the complex texture of the center and edge regions. Bar = 100 nm. (b) HRTEM image of monolayer-grown baryte crystal lying perpendicular to the [100] zone axis showing prominent (002) (0.358 nm) lattice fringes.

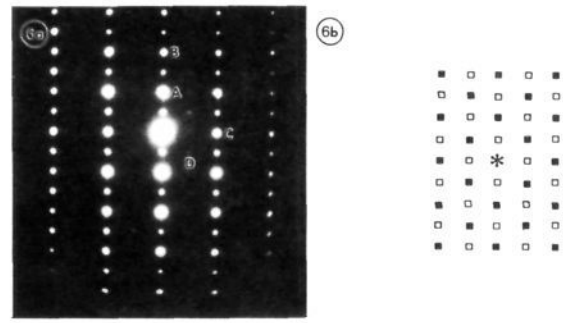

Figure 6. Single-crystal electron diffraction pattern obtained from an *n*-eicosyl sulfate nucleated crystal. The pattern corresponds to the [100] zone: reflection A = (020) (0.273 nm), B = (011) (0.434 nm), C = (002) (0.358 nm), D = (004) (0.179 nm). Angles (020) ∧ (002) = 90°, (020) ∧ (011) = 37°. (b) Drawing of diffraction pattern in (a). Additional reflections (□) corresponding to (001) (0.716 nm), (003) (0.258 nm), (005) (0.143 nm), etc.; (010) (0.546 nm), (030) (0.182 nm), etc., are also present.

and the nucleation density (1.3×10^2 crystals/mm^2) was significantly lower than that for *n*-eicosyl sulfate films. Viewed in TEM, individual crystals collected at t = 8 h were large (10 – 15 mm in length) and exhibited a complex dendritic "bow-tie" morphology comprising a series of triangular plates radiating from a central point (Figure 7a). The nucleation and growth properties of these crystals were determined by studying the structure, morphology, and crystallographic orientation of particles extracted from the Langmuir trough at earlier time points (e.g., t = 2–4 h). The immature crystals were elongated asymmetric disks (length = 3.27 mm, s = 0.79); one side of the particle had two smooth edges, whereas the other was roughened and hemispherical (Figure 7b). The two smooth edges correspond to the surface of the crystals in contact with the monolayer while the roughened side of the disks was formed by the crystals growing out into solution. With continued growth these crystals developed well-defined faces at the periphery of their long physical axis, and, often, a series of small triangular plates appeared along the roughened

(21) Vainshtein, B. K. In *Structure Analysis by Electron Diffraction*; Pergamon Press: Oxford, 1964.
(22) Kunzmann, P.; Eyring, L. *J. Solid State Chem.* **1975**, *14*, 229–237.

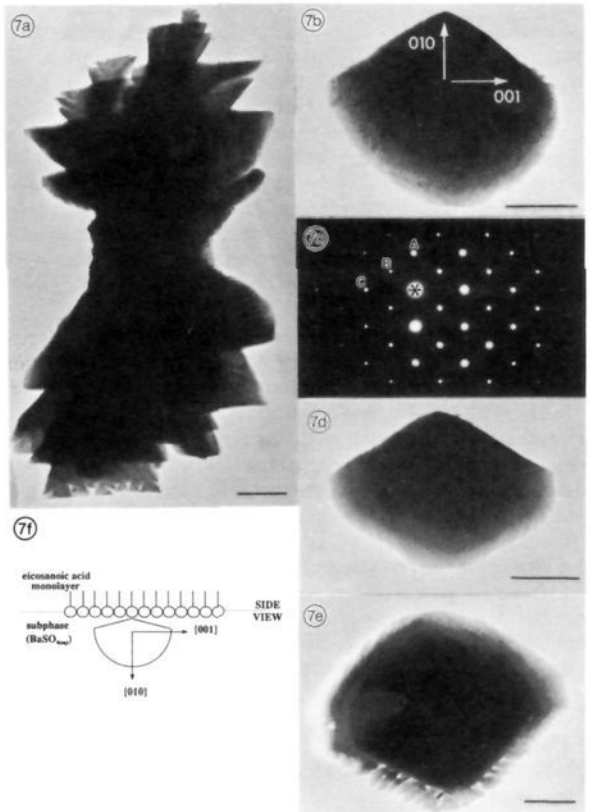

Figure 7. (a) TEM of a mature crystal of $BaSO_4$ grown under a compressed monolayer of eicosanoic acid. Bar = 1 μm. (b – e) TEM micrographs of immature crystals (Bars = (b) 500 nm, (d) 1 μm, (e) 1 μm). The single-crystal electron diffraction pattern corresponds to the [100] zone of $BaSO_4$ and was obtained from the crystal imaged in (b). (f) Schematic showing the relationship between the morphology of the crystals, their crystallographic ultrastructure, and their orientation relative to the monolayer.

hemispherical edge (Figure 7, d and e). The mature "bow-tie" morphology developed from the continued outgrowth of these small triangular elements.

The morphology of the crystals was such that single-crystal diffraction patterns were obtained only from immature crystals lying on their large side faces (see Figure 7, b, d, and e). In most cases the electron diffraction patterns corresponded to the [100] crystallographic zone of $BaSO_4$ (Figure 7c). The [001] axis was coincident with the long physical axis of the crystals, and lay parallel to the monolayer. The [010] crystallographic axis was oriented perpendicular to the plane of the monolayer, suggesting that the $BaSO_4$ crystals formed under eicosanoic acid nucleated on a (010) face (Figure 7f). The triangular outgrowths had large top and bottom faces of (100) index bounded by terminal (010) faces, and the long side faces were of {011} type.

Discussion

The data reported in this paper indicate that a compressed monolayer of the surfactant *n*-eicosyl sulfate promotes crystallization of $BaSO_4$ almost exclusively at the monolayer/solution interface. This effect is significantly reduced for monolayers of eicosanoic acid. The crystals orient with the (100) face aligned parallel to the organized organic surface generated by compressed sulfate monolayers, while the [010] direction is preferentially aligned perpendicular to carboxylate monolayers. In conjunction with previous studies on $CaCO_3$ nucleation under stearate monolayers,[3-9] the present results illustrate two important and interrelated features of monolayer-mediated crystallization: (i) highly ordered functionalized organic surfaces have the potential to catalyze inorganic crystallization, and (ii) interfacial matching is of key importance in directing crystal nucleation. Clearly, the effect is to redefine the energetic constraints to nucleation such

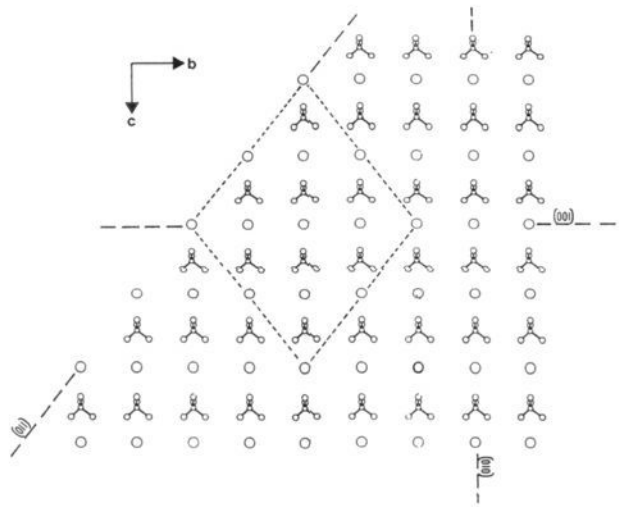

Figure 8. A computer generated drawing of the (100) face of barium sulfate.

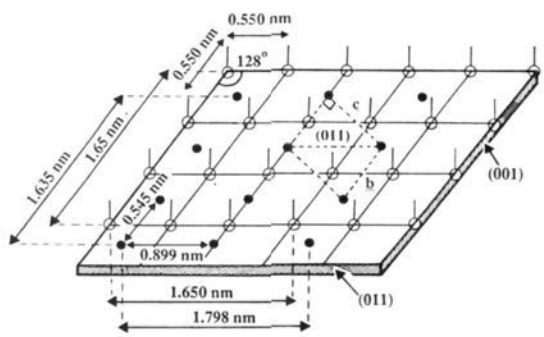

Figure 9. Schematic of the [100] zone of nucleation showing the potential cation binding motif developed by the interaction of Ba^{2+} (large circle) with the sulfate-monolayer.

that crystallization at the monolayer surface is favored kinetically against precipitation in bulk solution. In addition, the crystallographic ordering of the monolayer-induced particles implies that this kinetic control over nucleation is achieved through the translation of specific structural and chemical information at the organic–inorganic interface. In this respect, the organic surface must act to stabilize the transition state (nucleus) by providing an interfacial structure commensurate with the geometric and stereochemical requirements of the (100) crystal face of $BaSO_4$.

What aspects of the (100) face could be simulated by the interaction of barium and sulfate ions with an *n*-eicosyl sulfate monolayer? Surfactant monolayers are known to adopt hexagonal or pseudo-hexagonal lattices when compressed,[23-25] and it is assumed that monolayers of *n*-eicosyl sulfate assume this packing conformation under similar conditions. Superimposition of a hexagonal lattice of sulfate headgroups on the (100) face of $BaSO_4$ provides only a limited geometric match (Figure 8). The interheadgroup spacing of 0.55 nm is close to the coplanar Ba–Ba distances (0.545 nm) along the (010) direction of the (100) face, but no such relationship exists along the [001] since the Ba–Ba distances are significantly smaller than the corresponding spacings (1.0 nm) of the hexagonal unit cell. Rhombic distortion of the hexagonal angle to 128° (the angle between the [010] and [0$\bar{1}$1] axes), however, provides a much better matching in two dimensions. The Ba–Ba distance (0.899 nm) along the ⟨011⟩ direction is approximately 1.5 times that of the interheadgroup spacing.

(23) Dutta, P.; Peng, J. B.; Lin, B.; Ketterson, J. B.; Prakash, M. *Phys. Rev. Lett.* **1987**, *58*, 2228–2233.
(24) Kjaer, K.; Als-Nielson, J.; Helm, C. A.; Tippman-Krayer, P.; Mohwald, H. *Thin Solid Films* **1988**, *159*, 17–23.
(25) Lin, B.; Boahanon, T. M.; Shih, M. C.; Dutta, P. *Langmuir* **1990**, *6*, 1665–1667.

The Ba^{2+} ions could be accommodated provided that a supercell containing two different motifs was possible at the sulfate headgroups. One feasible arrangement is shown in Figure 9. The presence of two different sites would reduce the symmetry of the nucleated (100) face, and this could explain the occurrence of additional reflections in the electron diffraction patterns (see Figure 6).

The potential lattice matches (monolayer coordinates versus crystal lattice spacings) along the ⟨011⟩ and [010] directions are very high (97% and 94%, respectively). However, the {011} edge could be preferentially stabilized at the monolayer because the barium cations are spread at long distances (0.899 nm) in this face which could minimize neighboring cation–cation electrostatic repulsion. This may account for the predominance of rhombic domains in the central region of the crystals although other factors should be considered (see below).

A good potential lattice match exists in two dimensions between the morphologically stable (001) face (0.545 nm × 0.878 nm) and a putative hexagonal array of sulfate headgroups. The fact that this face is not nucleated suggests that an epitaxial relationship, although important, is not the primary factor in determining crystal orientation. Crystal faces are characterized not only by a series of repeating geometric patterns but also by the unique stereochemical orientation of the constituent ions or molecules in each plane. In this regard, the (001) and (100) faces of $BaSO_4$ have distinct differences in the stereochemical conformations of the sulfate anions. The sulfates exposed at the (100) face are positioned such that the C_2 axis of the tetrahedron is parallel to the surface while this symmetry axis is perpendicular to the plane of the (001) faces (Figure 8). The former is very similar to that of the alkyl sulfate headgroups at the monolayer/solution interface with the result that the association of Ba^{2+} with the ionized organic surface establishes a pseudo-morphic motif which is analogous to the (100) faces of the barium sulfate unit cell (Figure 8). It is this mimetic motif which generates the necessary template for the induction of oriented nucleation. No such stereochemical complementarity exists, for example, at the (001) face.

A unique feature of the $BaSO_4$ crystals grown under the sulfate monolayer is the rhombic texture of the (100) face in contact with the organic surface (see Figures 4c and 6). The presence of the unicharged {011} side faces which are generally unstable in solution indicates that these planes are preferentially stabilized during crystal growth parallel to the monolayer/solution interface. The occurrence of polar faces is usually related to habit modifications by site-specific additives which stabilize the faces through a charge neutralization process.[26,27] Additive-mediated habit modifications of $BaSO_4$ and isostructural $KClO_4$ leading to expression of {011} faces have been reported.[28,29] In the present system the most obvious candidate would be solubilized surfactant. Indeed, {011} faces are expressed when barium sulfate is precipitated in the presence of sodium dodecyl sulfate as an additive to the crystallization media [Hopwood, J.; Heywood, B. R.; Mann, S. Unpublished data]. However, the absence of hysteresis in the isotherms during compression negates possible solution effects[30] and suggests that the direct adsorption of the compressed monolayer onto the {011} faces merits consideration. Given the charge density of the {011} faces, it is envisaged that the surfactant sulfates would bind strongly to the close-packed barium ions (nearest-neighbor separation (Ba–Ba) = 0.56 nm) and induce the necessary surface relaxation processes to stabilize these lattice planes. These effects may be enhanced by stereochemical considerations since the monolayer headgroups have the capacity to undergo some restricted rotation around the carbon–oxygen bond and orient with their C_3 axis of symmetry lying parallel to the plane of the air/water interface,[17] a conformation which is analogous to the stereochemistry of the sulfates in the {011} surfaces (Figure 8). As the crystals continue to grow into solution, interactions of this type will be reduced and the crystals will develop the rectangular morphology observed in the control crystals.

The importance of stereochemical complementarity is further illustrated by the crystallization experiments with eicosanoic acid monolayers. In this case, crystal nucleation on the (010) face is probably mediated by charge accumulation, since there are no commensurate lattice coordinates between the monolayer and these faces, and certainly no stereochemical correspondence between the carboxylate headgroups of the surfactant and the sulfate anions in the (010) faces which lie with their C_2 axis parallel to the plane of the face. Interfacial charge accumulation has been cited as a key element in the process of crystal nucleation and growth under amorphous films where the facility for structural and stereochemical correspondence is absent [Heywood, B. R.; Mann, S. Unpublished data]. The complex dendritic morphology of the crystals is most likely to be the result of spatially restricted interfacial growth coupled with rapid growth into bulk solution (Figure 7a). Some realignment of the crystals may occur at the interface as the center of gravity shifts with continued growth, and this would then favor new growth directions as the contact of the monolayer with the crystal surfaces changes. The end result is the development of numerous outgrowths from an irregular central feature.

In summary, the monolayer-induced oriented nucleation of inorganic crystals such as $BaSO_4$ and $CaCO_3$[3-9] depends critically on the ability of the organic surface to mimic both the lattice geometry of cations and stereochemistry of oxyanions in specific crystal faces. Similar arguments have been presented for the selected interaction of molecular additives with crystal faces in studies of tailored crystal morphology.[12,29,31] These observations are relevant to current ideas in biomineralization where functionalized organic surfaces are considered to play a key role in the nucleation of many different types of inorganic materials. In particular, we note that $SrSO_4$ crystals in the marine acantharian *Phyllastaurus siculus*, and the colonial radiolarian *Sphaerozoum punctatum*, show morphologies consistent with nucleation on a (100) face.[32,33] As $SrSO_4$ is isomorphic with $BaSO_4$, it is conceivable that sulfate-functionalized macromolecules could be responsible for controlled nucleation in these biological systems. The exact composition of the organic matrices associated with the biominerals in these Protozoans is unknown, but the occurrence of sulfate-rich carbohydrates has been reported in some biogenic mineralization systems.[34]

Acknowledgment. We gratefully acknowledge the financial support of BP International Ltd.

(26) Rajam, S.; Mann, S. *J. Chem. Soc., Faraday Trans.* **1991**, *24*, 1789–1791.
(27) Titiloye, J. O.; Parker, S. C.; Ogusthorpe, D. J.; Mann, S. *J. Chem. Soc., Faraday Trans.*, in press.
(28) Buckley, K. *Faraday Trans.* **1949**, *5*, 243–254.
(29) Black, S. N.; Bromley, L. A.; Cottier, D.; Davey, R. J.; Dobbs, B.; Polywka, L. A.; Rout, J. E. *J. Chem. Soc., Faraday Trans.*, in press.
(30) Gaines, G. L., Jr. In *Insoluble Monolayers at Liquid-Gas Interfaces*; Prigogine, I., Ed.; 1966.
(31) Mann, S.; Didymus, J.; Sanderson, N. P.; Heywood, B. R.; Aso-Samper, E. J. *J. Chem. Soc., Faraday Trans.* **1990**, *86*, 1873–1880.
(32) Wilcock, J. R.; Perry, C. C.; Williams, R. J. P.; Mantoura, R. F. C. *Proc. R. Soc., London, Ser. B* **1988**, *233*, 393–405.
(33) Hughes, N. P.; Perry, C. C.; Anderson, O. R.; Williams, R. J. P. *Proc. R. Soc., London, Ser. B* **1989**, *238*, 223–233.
(34) Greenfield, E. M.; Wilson, D. C.; Crenshaw, M. A. *Am. Zool.* **1984**, *24*, 925–32.